45
Copy

NASA CR-66276

PROPERTIES OF POWDER GROUND IN ULTRAHIGH VACUUM

P. Blum
J. R. Roehrig
M. J. Hordon

March 1967

Prepared under Contract No. NAS1-5347, Task 2 by
Norton Exploratory Research Division
NATIONAL RESEARCH CORPORATION
Cambridge, Massachusetts

for

NATIONAL AERONAUTICS AND SPACE ADMINISTRATION

ABSTRACT

A comparison is made between the properties and behavior of basalt powder ground in vacuum and in air. The grinding apparatus is also described.

TABLE OF CONTENTS

LIST OF ILLUSTRATIONS

PROPERTIES OF POWDER GROUND IN ULTRAHIGH VACUUM

By P. Blum, J.R. Roehrig, M.J. Hordon

SUMMARY

This Final Technical Report covers the research program conducted by the Norton Exploratory Research Division of National Research Corporation under Contract NAS1-5347, Task 2, for the National Aeronautics and Space Administration, Langley Research Center, Hampton, Virginia, during the period August 24, 1965 to August 23, 1966.

Apparatus has been constructed for the comminution of igneous rock in ultrahigh vacuum. This was to allow determination of the properties of powders produced with atomically clean particle surfaces for application to lunar soil research. Rock components were mutually abraded; configurations and motions maintained an open grinding design to facilitate pumping of released gas and they allowed powder contact only with newly abraded rock surfaces prior to collection.

Basalt powder was thus produced while maintaining pressures in the low 10^{-9} and 10^{-8} Torr ranges. This required extensive rock baking, prior to comminution, causing a 0.66% weight loss. The powder, both free and compressed, displayed greater self adhesion and greater adhesion to solid rock and to metal surfaces than did powder produced at atmospheric pressure. Powder compressed during grinding adhered to vertical rock walls above the grinding interfaces, yielding self supporting flakes 1/7 inches wide; uncompressed powder accumulated on the underside of the rocks. No air ground counterparts to the latter existed. On the collecting pan, free powder formed angular, gravel-like aggregates. In air, aggregates were also formed, but in smaller amounts and were spherical in shape. The above results suggest that many of the "rocks" in the Surveyor and Ranger photographs may be powder aggregates.

Desirable improvements in comminution and collection methods are discussed, as well as methods for quantitative measurements of powder strength in vacuum.

INTRODUCTION

Preparation requirements for landing men on the moon have greatly intensified interest in the nature of the lunar surface. The need for concern about lunar soil, in particular, was

perhaps first made evident by estimates that unconsolidated dust over a mile deep may exist, caused by billions of years of meteoritic bombardment and pulverization. Anxiety over the drastic implications of this situation has greatly ebbed since the landing of Luna 9 and Surveyor I. However, the strength characteristics of lunar soil remain essentially unknown. There is no direct knowledge of soil shear strength, coefficient of friction, cohesion or of bearing capacity as a function of footing size and environment (e.g. mineralogy and soil depth). Bearing capacity has been determined for but one set of conditions.

This report describes a preliminary investigation into the properties of lunar soil, i.e. of comminuted igneous rock, by simulating what is believed to be an especially critical factor in determining its strength. This is the comminution of the rock in ultrahigh vacuum. Previous simulation studies and the need for vacuum comminution are discussed in the following section.

RATIONALE OF VACUUM COMMINUTION

A number of studies have been performed in recognition of the possibly significant effect which the lunar vacuum environment, which is about 10^{-10} Torr, may have on rock powder properties. Salisbury et al[1] sifted numerous kinds of igneous rock powder in vacuum in the 10^{-10} Torr range and found greater adhesion than when sifted at atmospheric pressure; this was evidenced primarily by a greater angle of repose. Halajian[2] tumbled rock powders of several types including basalt in the low 10^{-10} Torr range and also found sticking. Vey and Nelson[3] performed quantitative shear strength tests on silicon flour and olivine sifted at pressures from atmosphere down to the low 10^{-9} Torr range. Results here were mixed but increases predominated both in cohesion and in the coefficient of friction. Bernette et al[4] did a quantitative bearing capacity study on olivine basalt at 10^{-6} Torr and at this pressure found little strength differences from that at atmosphere. Wong and Kern[5] conducted both bearing capacity tests and shear tests in the 10^{-6} Torr range on pumice and on quartz sand and also appeared to find little strength difference in the two environments, except for a decrease of

quartz shear strength in vacuum.

The trend of the above studies appears to be that of a moderate powder strength increase in vacuum, when the latter approaches the ultrahigh vacuum range. This is consonant with the generally accepted requirement for vacuum adhesion, the increase in surface atomic cleanliness resulting from the scarcity of contaminating environment gases. It must be indicated, however, that if in simulation experiments, rocks are crushed in air, the powder will adsorb contaminating gases during comminution. Some of the gas layers resulting will remain even in ultrahigh vacuum (UHV). The surfaces will therefore neither simulate those expected to exist on the lunar surface nor will they be atomically clean. Only small adhesional differences from the behavior in atmosphere could therefore be expected.

Attempts were made by Salisbury and Halajian to overcome this problem. In the latter's work rocks were baked at elevated temperatures in vacuum subsequent to pulverization to desorb the gases. In Salisbury's experiments, rocks were ground in argon, because it is inert, and subsequently outgassed in UHV. Evaluation of these methods indicates, however, that surface cleanliness resulting from either may still differ considerably from that on the moon's surface.

Crushing rock in an inert atmosphere, while lessening atmospheric contamination (depending on the purity of the gas, among other factors), will nonetheless trap considerable amounts of gas that is released from the rock itself during pulverization, including water vapor. These gases will then be preferentially adsorbed within the inert atmosphere.

As regards subsequent outgassing in UHV, even by baking, work performed by Ham[6] is pertinent. He observed that metals ruptured in high vacuum welded when rejoined; however, the weld strength diminished considerably with intervening exposure time. Fig. 1, from Ham's paper, records the cohesion reduction against time and pressure at 150°C; components were compressed near their yield strength for the times indicated. The cohesion reduction with exposure occurred even at 500°C but with a diminished rate. Welding was attributed to the cleanliness of the surfaces freshly ruptured in high vacuum, cohesion reduction to gradual contamination by residual gases in the vacuum chamber. Therefore, while thermal degassing in UHV may be

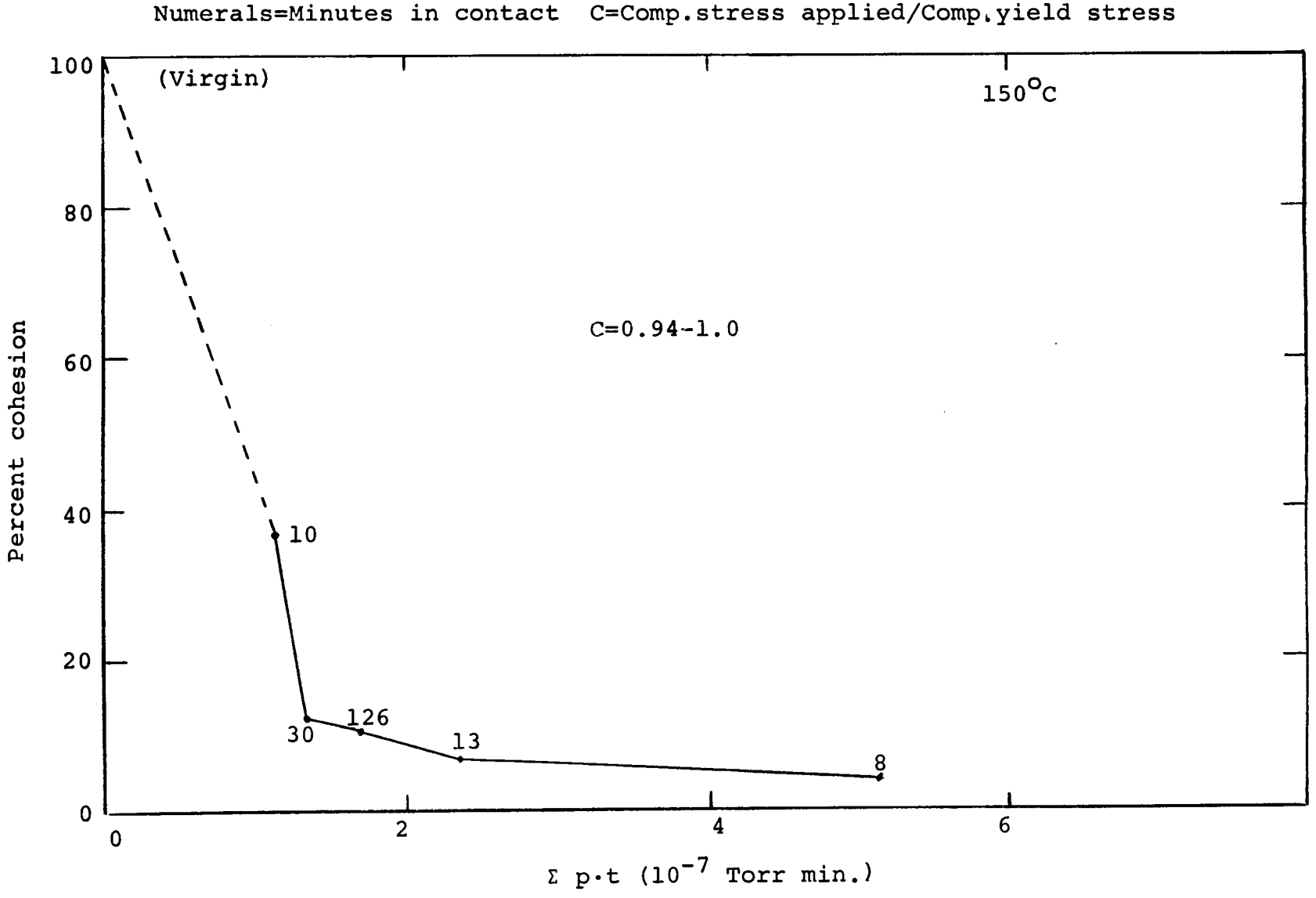

FIG. 1 Per cent cohesion of type 1018 Steel (Ham[6])

a useful cleaning technique, it appears unlikely that contaminated surfaces, e.g., the aforementioned rock powders, can be degassed completely enough to approach the atomic cleanliness of those produced in vacuum.

It may be concluded that the best approach is the reduction of rock to powder directly in UHV. As regards the production of atomically clean particle surfaces, this more closely simulates lunar comminution conditions than have those of previous experiments discussed above and permits observation of whether silicate powder thus produced has significantly different soil properties, e.g., regarding adhesion and friction. (P.R. Bell[7] has very recently published work on the vacuum comminution of olivine in a ball mill at 2×10^{-7} Torr, showing evidence of considerable adhesion. Pertinent work is now also in progress by J. A. Ryan[8] on the vacuum cleavage of single silicate crystals; specimens cleaved at 1×10^{-10} Torr show considerably greater adhesion when brought in contact in vacuum than if previously cleaved in air).

SPECIMEN SELECTION

A literature search was conducted to ascertain which rock types are believed representative of the lunar surface. Under simulated solar wind bombardment, Rosenberg and Wehner[9] found powdered basalt (of 2 - 10μ particle size) to develop albedo and relective characterisitics most similar to the lunar surface. Green[10] has tabulated a version of probable lunar surface materials, among which basalt is prominent along with chondritic meteorites. Generally, however, it was found that rock chemical compositions are still unknown.[11,12] There is agreement only that the rock is igneous.

Among researchers investigating the effect of vacuum on simulated lunar soil (discussed previously) the following materials were used: Salisbury et al tested representatives of the entire ingeous rock series (obsidian, basalt, andesite, dunite and pyroxenite) plus a chondrite and a tektite with uniform results regarding powder adhesion. However, most of his results are illustrated with a dense black basalt. As noted

previously, Bernette et al used olivine basalt, Halajian also used basalt, Nelson and Vey used silicon flour and olivine, Wong and Kern used quartz and pumice.

Since basalt appeared to be most widely accepted and most used in simulation studies it was selected for initial studies. The basalt used is dense black, unweathered and is from Lintz, Rhenish Prussia. It was purchased from Ward's Natural Science Establishment, Rochester, N.Y.

The chemical composition of basalt, as of rocks generally, varies somewhat with geographical location and among samples within each location. However, the average basalt composition as given by Spock,[13] according to weight per cent for each oxide, is shown in Table I.

Table I. Average Basalt Chemical Composition (Spock[13])

Oxide	% Wt.	Oxide	%Wt.
SiO_2	49.06	CaO	8.95
Al_2O_3	15.70	Na_2O	3.11
Fe_2O_3	5.38	K_2O	1.52
FeO:	6.68	H_2O	1.62
MgO:	6.17	TiO_2	1.36
		P_2O_5	0.45

APPARATUS

Grinding and Collection

Fig. 2 shows, schematically simplified, a vertical cross section of the grinding components relative to the rest of the vacuum chamber. Both of the two grinding components are made of basalt. The inner one is essentially cylindrical with a

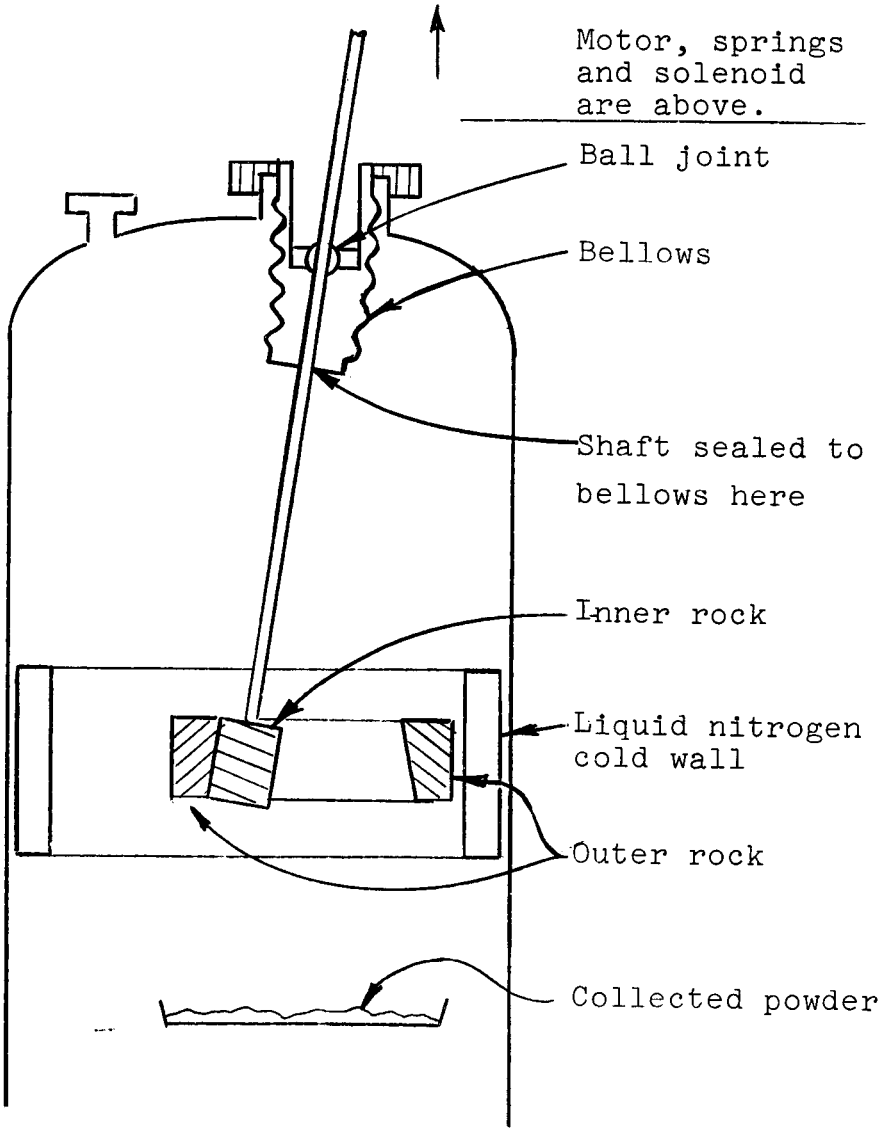

FIG.2. Simplified, cross-sectional sketch of rock grinding components relative to the rest of the vacuum chamber.

diameter of 2-1/4 inches and a thickness of 1-3/8 inches. It revolves abrasively about the inside surface of a fixed, torroidal shaped outer component, which has an inner diameter of 4-1/8 inches, an outer diameter of approximately 6 inches and a thickness of 1-3/8 inches.

The inner component is held by a shaft which is free to pivot in three dimensions by means of a ball joint. The ball joint is located in the center of a flexible stainless steel bellows. The shaft is attached and sealed to the bellows at the bottom leaving the ball joint outside the vacuum chamber. The stiffness of the bellows prevents the shaft and hence the inner grinding component from turning on its own axis. Springs acting against the shaft in the motor mount provide the mechanical grinding pressure. A motor moves the shaft about its pivotal point. The above motion and constraints cause the exposure of new, clean wall surfaces over the entire circumference of each component once every revolution. The inner component is also vibrated longitudinally with a displacement of 1/8 inch. The powder produced is collected in a pan directly below the grinding area.

The above grinding arrangement was designed to include the following benefits:

(a) The grinding is open. This is as opposed to a crushing procedure, or the rubbing of two flat surfaces together, or the rotation of one grinding component into another. The open design facilitates the pumping of gases released during comminution and thus helps to prevent particle contamination. This, in turn, helps simulate outgassing conditions during comminution on the moon.

(b) The open grinding design maintains itself by the even wearing of components.

(c) In their trajectories caused by the tangential grinding forces, abraded particles can bounce only against clean surfaces before falling into the collecting container.

(d) Particles proceed to the place to be tested immediately subsequent to grinding, thus avoiding contamination inherent in a separate and delayed collection procedure.

(e) The grinding system is "clean" in a vacuum sense by requiring a minimum of apparatus and crevices within the vacuum chamber.

(f) The use of two rock components instead of one rock and one grinding wheel was intended to eliminate two potential problems; grinding wheel contamination of the powder and grinding wheel clogging.

(g) Vibratory motion was included to prevent formation of a lip in the outer rock as the rock is worn away, thus preventing powder trapping and contamination, as well as preventing interference with the grinding operation.

Fig. 3 shows a simplified sketch of the motor mount and slide assembly. A 1/8 H.P. D.C. motor was used connected to a controller for varying speeds between 3.5 and 125 rpm. Mechanical forces between rock grinding interfaces was maintained at 10.5 lbs by the compressed spring in the slide assembly. A solenoid placed around the shaft was used to supply a slow vibratory motion, which was maintained at 0.4 cpm.

The collecting pan was placed 7 inches below the bottom surface of the rocks to permit viewing of the grinding operation from below and the formation of powder on the pan from above. The pan held a 200 gm weight for testing the effect of powder compression. It also held a vessel for confining powder, to test the effects of funneling, and a bridge over which powder could drape itself to assist observations of powder adhesion.

Vacuum Chamber and Pumping System

Fig. 4 shows a photograph of the apparatus less the electronic controls. The grinding motor and its mount rest on the vacuum chamber which in turn rests on the ion pump. The circular platform between chamber and pump supports an oven during chamber bakeout. The pump has an internal bakeout mechanism.

Fig. 5 shows an assembly drawing of the vacuum chamber which is 14 inches in diameter and 37 inches between upper and lower flange extremities. Two 4 inch diameter viewing ports at right angles and offset relative to each other are placed below the grinding area, which is walled off by a liquid

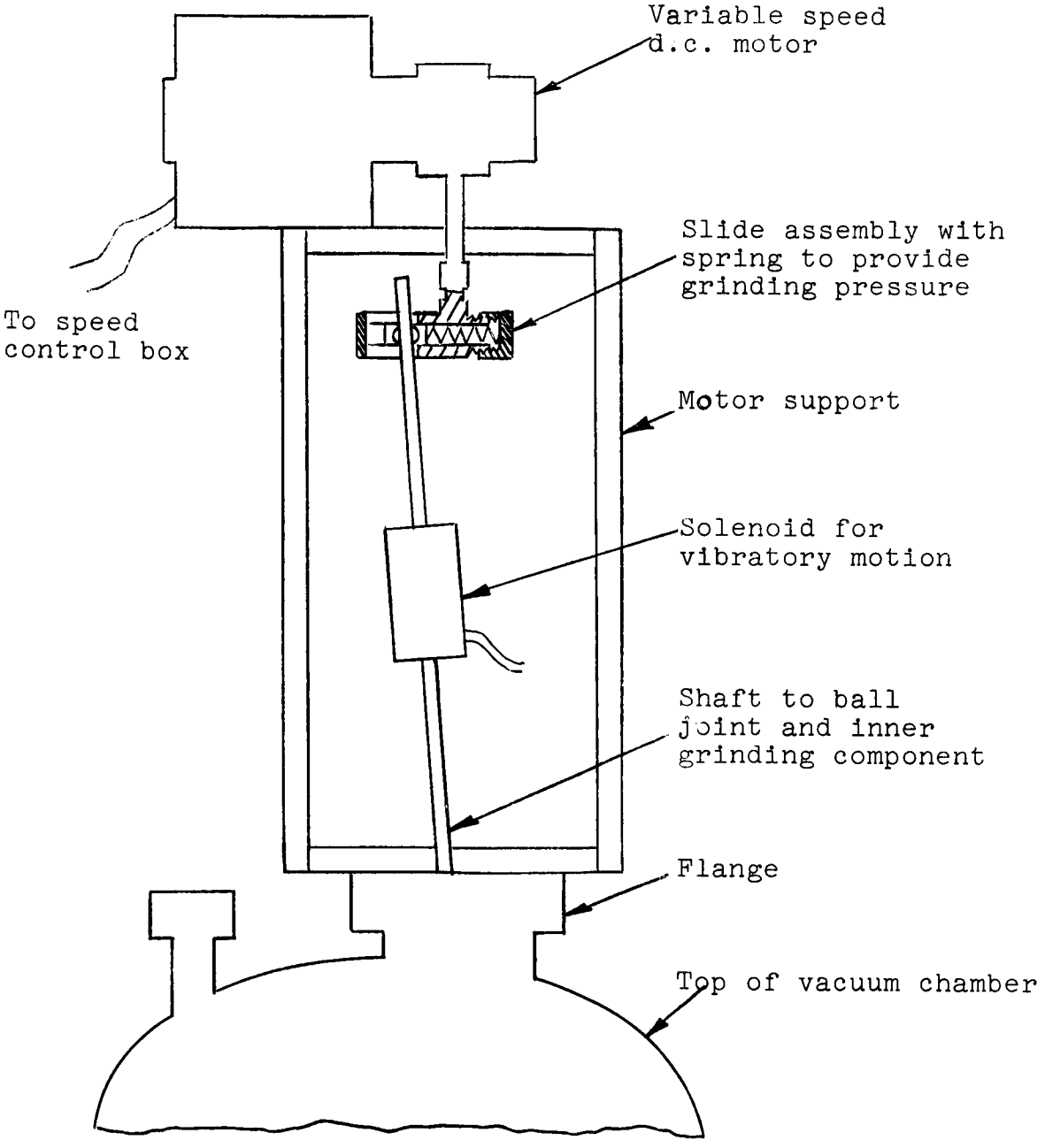

FIG. 3. Simplified sketch of motor mount, slide assembly and solenoid.

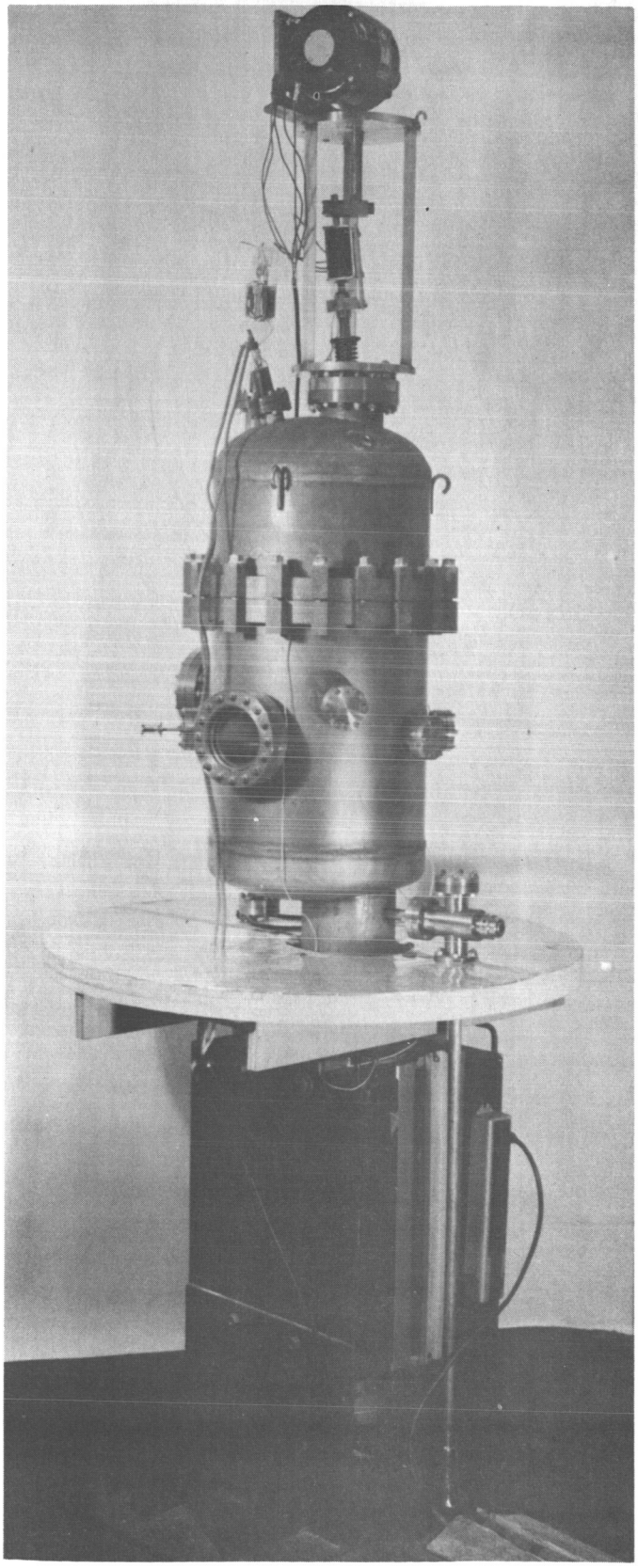

FIG. 4. Photograph of chamber, ion pump and motor mount.

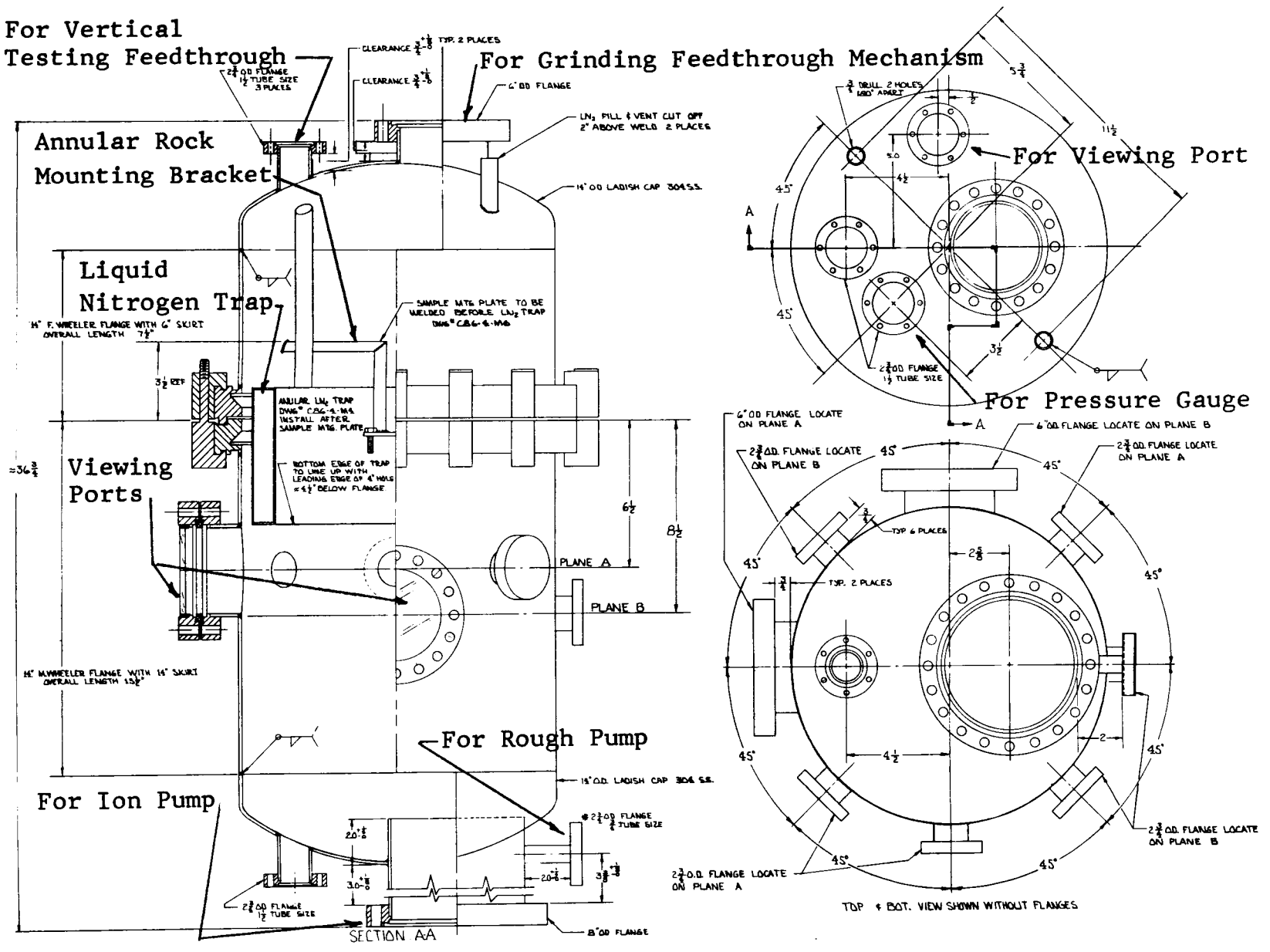

FIG. 5. Vacuum chamber assembly drawing.

nitrogen trap (discussed below). These permit both a view of powder on the pan and a view of the grinding operation. A third 1 inch diameter viewing port is at the top of the chamber for viewing from above. Of the two remaining flanges, one was used for attaching a pressure gauge and the other is reserved for attaching a vertical testing feedthrough when large normal powder testing forces are required. The 6 inch diameter flange at the top is for the grinding feedthrough mechanism. It is off-centered to allow room for the vertical testing.

A 17-5/8 inch flange divides the chamber to optimize accessibility and is as near to the center as is compatible with other requirements. The 8 inch flange at the bottom of the chamber attaches to the ion pump flange. A UHV valve is attached to the small flange at the right of the chamber labeled "for rough pump", as shown in Fig.5, and leads to the roughing manifold. Remaining small flanges about the circumference are reserved for manipulative devices and other future requirements. One such manipulative device, a prong working through a bellows, was used for placing the 200 gm weight on the fallen powder and for other qualitative tests.

To minimize gas trapping, all threaded nuts and bolts used inside the chamber were slotted and open loops of wire were used between flat mating surfaces.

Fig. 6 shows a schematic of the vacuum system. It was designed to provide a large pumping capacity. This was to enable maintenance of pressures approaching those of the lunar surface (10^{-10}Torr) during grinding while allowing a reasonable powder production rate. A diffusion pump would ordinarily be most efficient for this purpose except that diffusion pump oil (silicone oil) backstreaming can cause serious surface contamination difficulties. Due to its low vapor pressure, this contamination will not be indicated as a rise in chamber pressure. Such difficulties often arise even when cold traps are used between pump and chamber, unless they are very carefully designed. To avoid all suspicion of such difficulties, an ion pump was used. It was made by Varian and has a 400 lit/sec pumping capacity.

Table I showed that basalt contains 1.62% by weight of H_2O. While a portion of this will be chemically bonded and while rock prebaking will drive off a good deal of water, a considerable amount of H_2O could still be volatized during grinding. A nitrogen cold wall was therefore used in conjunction with the ion pump to condense water vapor released during grinding.

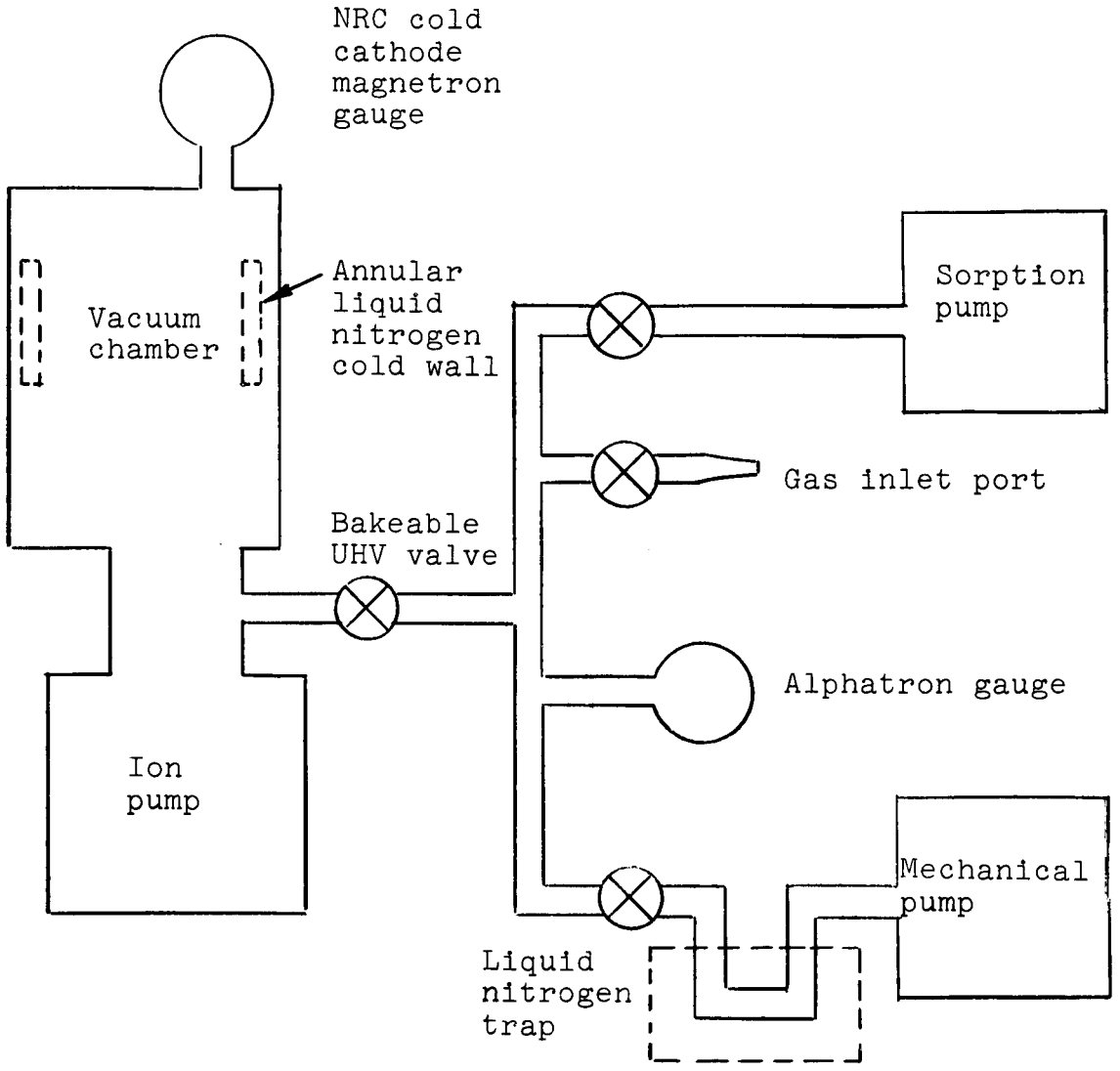

FIG. 6. Vacuum system schematic

The insufficiency of the ion pump and the requirements of the cryogenic pump are revealed as follows: Assume that during grinding there is volatized a rock weight fraction f of 0.0016 (i.e. 10% of the H_2O in the rock). Assume also that a pressure P of 10^{-9} Torr is to be maintained utilizing the ion pump's 400 liter per second pumping speed S. The time that would be required to grind a reasonable mass m of rock powder, e.g. 10 grams, can then be computed from the relationship

$$t = \frac{fmA}{MNPS} \qquad (1)$$

where the molecular weight of water M is 18 grams, the number of water molecules per Torr-liter N is 3.2×10^{19} (at $298^{\circ}K$) and Avogadro's number A is 6.02×10^{23}. Upon substitution,

$$t = 4.2 \times 10^{7} \text{ seconds} = 480 \text{ days.}$$

While assumption of an f of 0.0016 may be high, it is seen that the use of the ion pump itself could impose unreasonably long grinding time requirements. A nitrogen cold wall was therefore constructed with a calculated pumping speed of 22,000 liters per second. This reduces the estimated grinding time for the assumed conditions to about 9 days. The trap is cylindrical with a 12 inch diameter and a 7 inch height. It surrounds the rock grinding area; the intent was to permit as many released water molecules as possible to hit the cold wall before bouncing, to lessen their chances of contaminating the ground powder.

As shown in Fig. 6, a second liquid nitrogen trap was used between the mechanical pump and the rest of the system to prevent mechanical pump oil backstreaming. The latter does not pose the difficulties discussed for diffusion pump silicone oil, however, since the mechanical pump oil can be baked out before UHV pump-down and then valved off. It also does not have a low vapor pressure. The trap is used primarily to reduce the baking time. The chamber and ion pump were closed off from the roughing manifold by a Varian bakeable UHV valve. A sorption pump was attached to speed the pump-down time but was little used.

The roughing manifold pressure was monitored by an NRC Alphatron® gauge. UHV chamber pressure was monitored by an NRC cold cathode magnetron gauge attached at the top of the chamber. A cylindrical oven 34 inches in diameter by 48 inches in length, utilizing nine 1600 watt quartz lamps, was constructed for baking the chamber.

PROCEDURES, RESULTS AND DISCUSSION

Preliminary Experiments

Rock preparation. - The basalt was cut to the approximately desired shape with diamond core drills and diamond cut-off wheels by the Rock of Ages Corp., Barre, Vermont. Final shaping was accomplished by grinding rock components together in air in their final mounting position in the vacuum chamber. This provided contact over most of the thickness of the components.

It is well known that without baking a vacuum chamber and its components it is virtually impossible to attain ultra-high vacuum. It was found however that gas emanating from the basalt during a vacuum bake-out was too great to be handled by the ion pump. Rock components were therefore first baked in an oven at atmosphere to degas them. After several attempts with expendable pieces, procedures were established which allowed the specimens to be baked gradually to 400°C without shattering them.

Fig. 7 shows the percentage of rock weight loss as a function of time accompanying increased baking temperatures. The specimen charted is the inner component subsequently used for vacuum grinding. As might be anticipated, the rate of weight loss is greatest at the beginning of each new temperature setting and levels off towards the end of it. Approximately 0.65% of the rock by weight was volatized from each rock component. Because of the temperatures involved and the large percentage (1.62%) of H_2O in most basalts, this loss is attributed primarily to water vapor volatization. The huge amount of the latter that was observed supports the conclusion, discussed previously that powder still would be contaminated even if rocks were comminuted in an inert atmosphere.

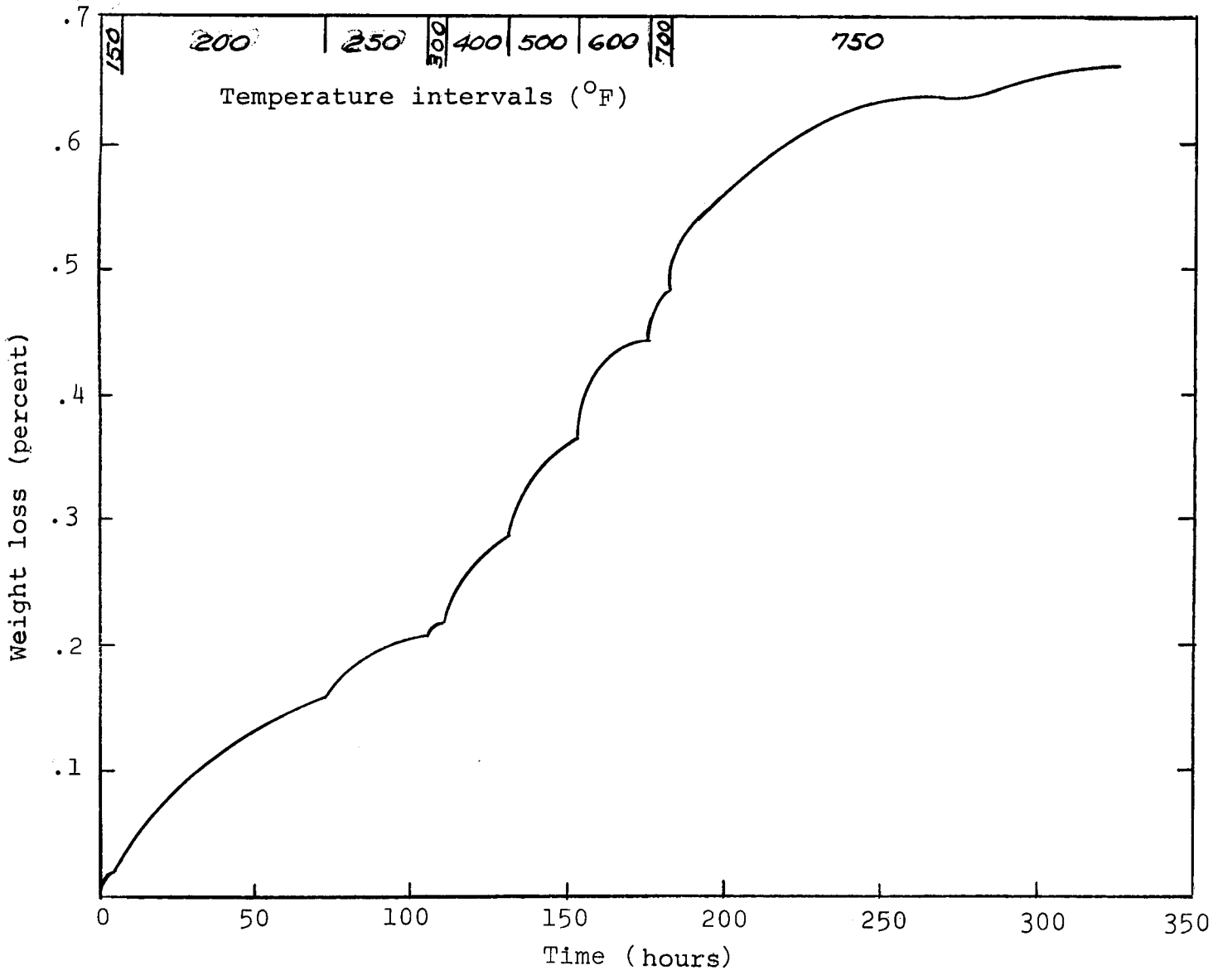

FIG. 7. Inner rock weight loss vs. time accompanying increased baking temperatures (shown in °F).

The rocks were again baked while under vacuum with the rest of the vacuum chamber and its components. The baking procedures ultimately allowed chamber pressure, with rock components assembled, to reach 7×10^{-10} Torr before grinding. The latter was achieved with liquid nitrogen in the trap.

Comminution in air. - Vacuum grinding was preceded by experimentation in air with rock on rock abrasion. Powder production rates as a function of grinding parameters were determined, as well as resultant size distributions as a function of rock type.

Particle size distributions resulting from grinding basalt, olivine basalt and pumice, each upon themselves is shown in Table II. Sizes were determined by visual counting using an optical microscope. A standard quartering process was used to obtain representative specimens. Three possible candidate materials are thus seen to give a size distribution by means of self abrasion, which is commensurate with the micron range believed existent on the lunar surface. Pumice is seen to give the coarsest distribution and basalt the finest. Olivine basalt, which had the coarser grain structure of the two basalts gave the coarser distribution. Results are for grinding speeds of 0.5 surface feet per minute; mechanical grinding pressures were 3 psi for the basalt and olivine basalt and 0.1 psi for pumice. Corresponding production rates were 0.6 grams per hour for basalt and olivine basalt, 300 grams per hour for pumice. These powders were produced by rotating a cylindrical rock in place of a grinding wheel against a second, flat, rock in a conventional grinding manner.

Table II. Percent Number Distribution of Air Ground Particles

Rock Powder	Size Range (microns)					
	<.8	0.8-3	3-5	5-15	15-20	50-200
Olivine Basalt	35%	60%	5%			
Basalt	68%	32%				
Pumice	61%*		4%	13%	12%	9%

*51% were between 0.1 microns, 10% between 1-3 microns

Production rates and size distributions were again ascertained in air for the vacuum comminution method. This is described in the section which follows.

Air Grinding by the Method Used in Vacuum

Subsequent to the vacuum grinding experiments, to be discussed subsequently, grinding was performed at atmospheric pressure under otherwise identical circumstances. Grinding proceeded for the same length of time as in the second vacuum grinding experiment and the rock components employed were those previously used in vacuum. The purpose was to compare the effects of the gaseous environment on critical phenomena. The results obtained at atmosphere are discussed in subsequent sections as they relate to observations made on vacuum ground powder. Grinding at atmospheric pressure is henceforth referred to as air grinding.

First Vacuum Grinding Experiment

The vacuum chamber containing the rock components ready for grinding was initially at a pressure of 7×10^{-10} Torr, after which the pressure suddenly rose to 2×10^{-9} Torr and stabilized. This rise was traced to a small leak in the liquid nitrogen cold wall. Pressure then rose as grinding was commenced and increased with grinding speed. It remained near 7×10^{-8} Torr at 60 rpm. Powder initially produced fell into the pan. Powder subsequently produced accumulated on the rock grinding interfaces. The latter adhered despite continual abrasion and vibration. Eventually, further abrasion produced no additional powder. Grinding was allowed to proceed for one hour.

A photograph of the rock grinding components subsequent to vacuum grinding is shown in Fig. 8. It was taken through a viewing port with the components still under vacuum. The inner component is shown extended below its grinding position. (In an unsuccessful effort at dislodging the powder by manually knocking rock components together, a supporting pin broke resulting in bellows extension and hence inner component extension). The adherent powder is the light material on the interfaces. It has the appearance of smeared clay. This pattern remained unaltered as the rocks ground against each other. The unevenness of the pattern is at least partly

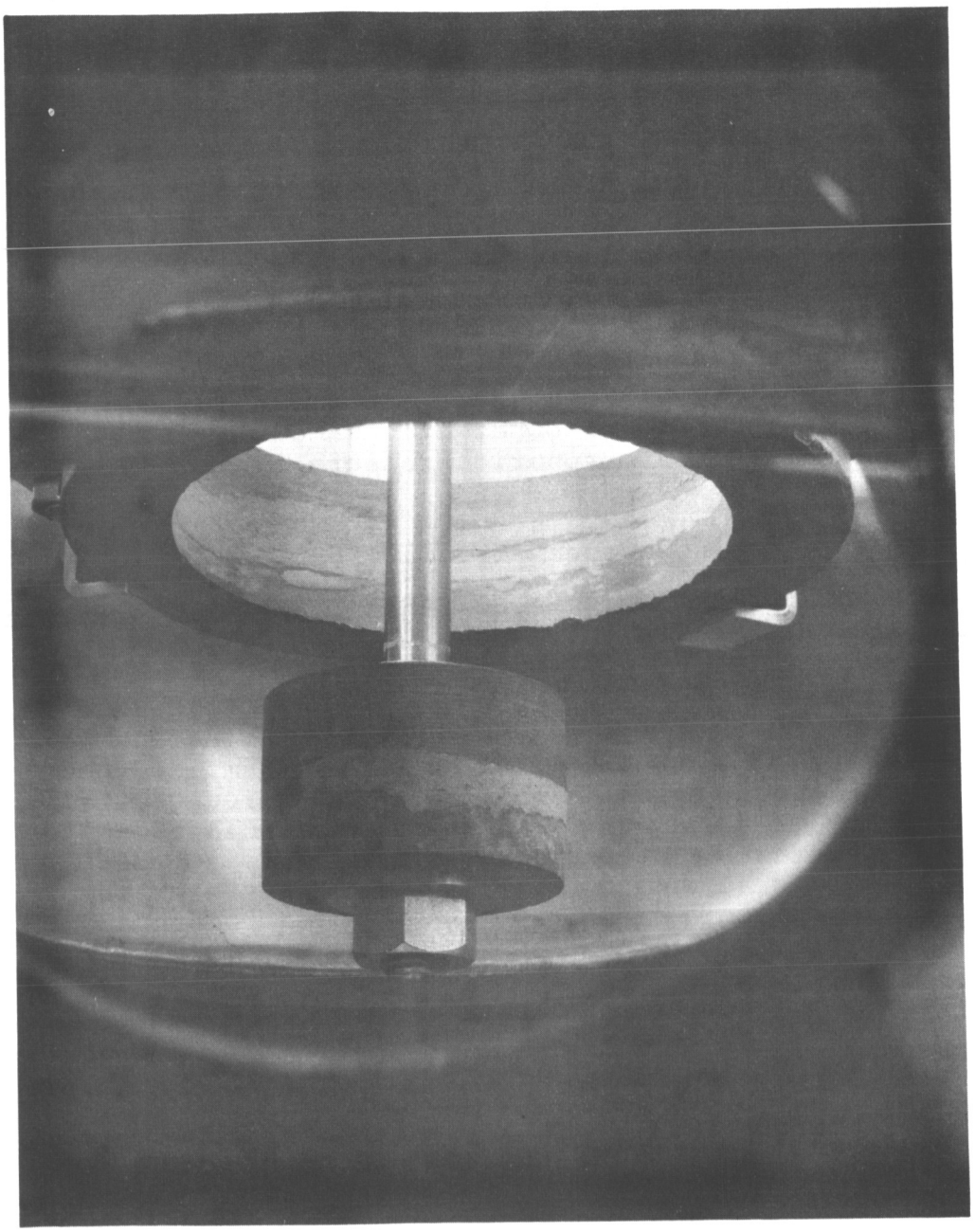

FIG. 8. Grinding components and adherent powder after the first vacuum grinding experiment.

attributed to a slightly uneven alignment of rock components and hence lack of contact along the full thickness of each rock. This situation was remedied in the second vacuum grinding experiment.

The powder remained adherent following release of the chamber to atmospheric pressure. Some of the powder appeared to be several tenths of a millimeter thick. Vigorous rock tapping failed to dislodge it even in air. However, it could be taken off as powder by repeated rubbing with the finger or as flakes several millimeters in diameter with a knife. The flakes were strong enough to remain self supporting when handled.

Second Vacuum Grinding Experiment

Preparation.- In preparation for the second experiment, the following steps were taken: (1) The liquid nitrogen cold wall was repaired. (2) Rock interfaces were mutually abraded in air after final assembly to eliminate the misalignment experienced in the first experiment. (3) Rock components were baked under vacuum for several days. These steps were taken, respectively, to lower initial chamber pressure, to reduce powder contamination caused by contact with unabraded, unclean rock and further to reduce outgassing during grinding.

Pressure variations with grinding. - A blank-off pressure of 1.9×10^{-9} Torr, with liquid nitrogen in the cold trap, was indicated before the start of grinding. Although the pressure was virtually the same as obtained in the first experiment, no cold trap leak was evident; the higher than previous blank-off pressure was attributed to a gradual deterioration in ion pump effectiveness.

Pressure rose when grinding commenced and increased with grinding rate, as noted in the first experiment. Grinding was sustained at 60 rpm except for momentary excursions to other values between 3.5 and 120 rpm. Longitudinal vibrations were maintained at 0.4 cpm. Pressure at 60 rpm initially rose to 2.6×10^{-8} Torr, which was almost half a decade lower than in the first vacuum grinding experiment. This improvement is attributed to the additional rock baking in vacuum.

Pressure decreased with time with sustained grinding regardless of rate. Fig. 9 shows a plot of pressure vs. grinding time at 60 rpm over the approximately 17 hours that grinding was in effect. Approximately 10 minutes of grinding, predominantly at lower speeds, followed by approximately 10 minutes of rest preceded the record illustrated.

Pressure is seen to drop rapidly with time after about two minutes of grinding. After about an hour, it begins to level off and approaches the system pressure existent before grinding. This drop in chamber pressure is attributed to obstruction of gas released during grinding by the gradual build up of powder adhering to the rock interfaces.

Behavior of powder in vacuum. - Streaks of adherent dust could be seen on rock interfaces after about a dozen initial grinding revolutions. At this time the grinding rate was 10 rpm and the pressure was 4×10^{-9} Torr. Powder adhered first to the bottom of rock interfaces and then proceeded up the sides.

Loose dust was evident in the pan during the first few minutes of grinding. Dust collecting in the pan within the first half hour (at 60 rpm) were spread primarily in small pools which were typically several mm in diameter. These appeared to be flat aggregates. A small fraction of the powder was observed "dancing" at the side of the pan, however, due to pan vibrations; this powder formed small round aggregates a fraction of a mm in diameter. The latter configuration appeared to be an indication of contaminated powder. Thus it was observed that in the pan, initially, part of the powder appeared clean and a smaller part contaminated; much of the latter was probably from the rock's first monolayer.

After 17 hours of grinding, when grinding was terminated, the number and size (up to 2 mm) of spherical "dancing" aggregates increased considerably. This is believed due to increased contamination of much of the powder. These aggregates resemble those produced by air grinding. Powder in the pan moved easily in response to a push by the manipulator.

Clumps of powder about 30 mm^3 each adhered to the underside of the outer rock in two locations. However, about an hour after grinding most of this material began falling off.

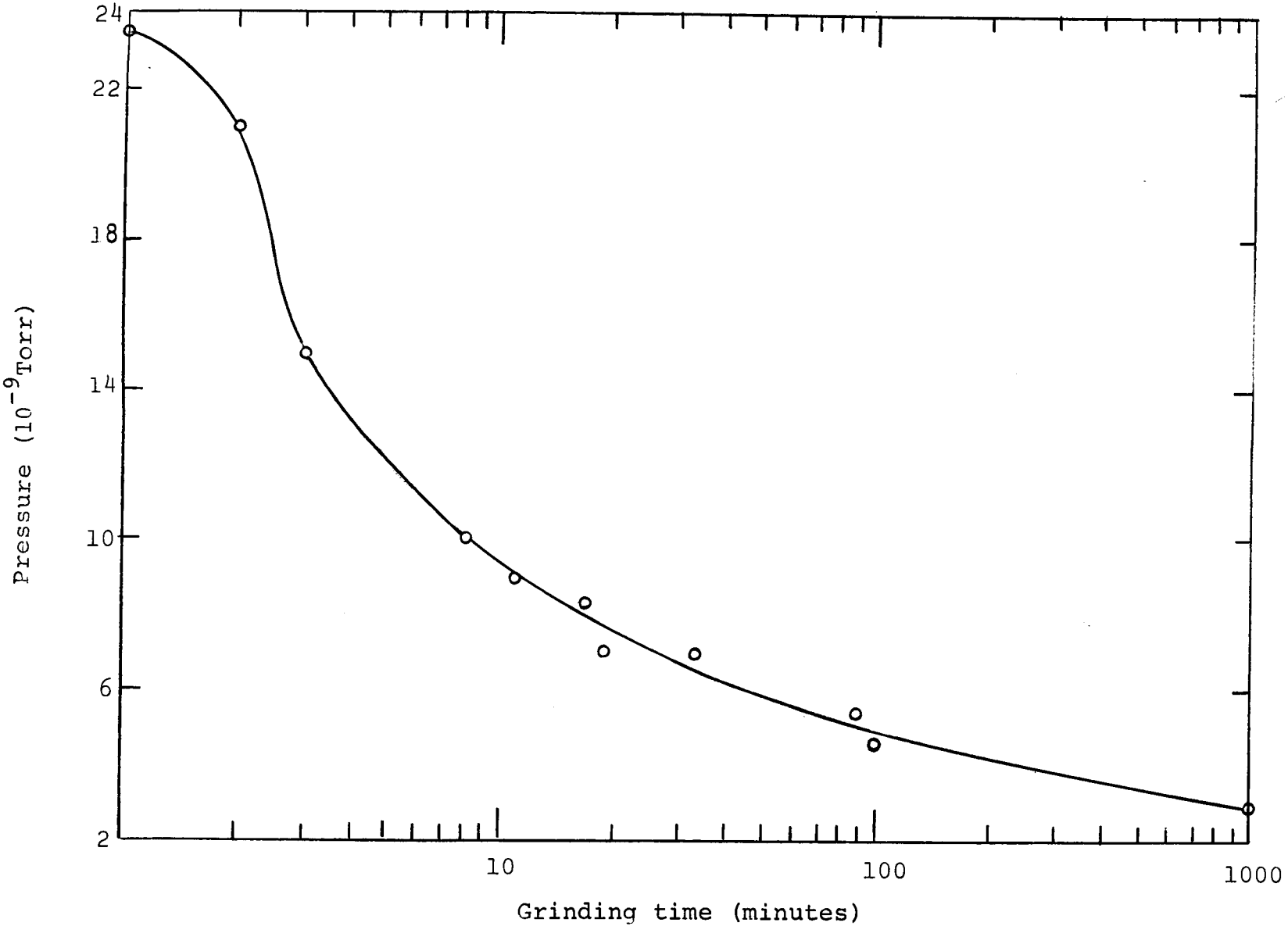

FIG. 9 Chamber pressure vs. time during grinding.

Apparently the powder eventually got too heavy to adhere amidst vibrations caused by rock grinding.

Fig. 10 shows a view of rock grinding components in vacuum through one of 4 inch ports just before the commencement of grinding. Fig. 11 shows the same view after about 1-1/2 hours of grinding. Chamber pressure was 5×10^{-9} Torr. At this stage, adherent powder has built up part way up the sides of the rocks. A small amount of adherent powder on the underside of the outer rock remains and can be seen at the rear of the outer rock. (The nitrogen cold wall obstructs part of the view of the outer rock.)

The powder production rate appeared to ebb with time but not to the extent observed in the first experiment. After grinding for 17 hours, adherent powder could be seen over the entire rock grinding interface, which existed about 3/4 of the way up the sides of the rocks. It has an even but unsymmetrical boundary. Fig. 12 shows one view of this area. The line separating the abraded and unabraded wall areas is evident. Also evident is the existence of powder above this line, which has apparently been shoved to this location. Fig. 13 presents another view, with the inner component moved to the left. The dark spot midway down the wall of the inner component contacted a crevice in the outer rock and hence remained unabraded and free of powder. A larger quantity of powder above the area of mutual abrasion is evident in this photograph, including some on the inner component.

Fig. 14 is a view of the pan, the manipulator, and the weight in vacuum after all grinding has been terminated. The weight had previously been placed on some of the powder to determine the effect of a known compression. Due to vibration, it slid to a position near the port and it is therefore in the foreground. The smeared powder it produced can be seen to the left of the weight. The powder seen resting on the manipulator arm was sufficiently adherent to resist falling or otherwise displacing itself under the action of vigorous and repeated vibrations of the arm, through the bellows. In air grinding, powder on the manipulator arm was easily dislodged under this action.

Powder behavior after release to atmospheric pressure. - After completion of 17 hours of grinding, the powder was left under vacuum at 3×10^{-9} Torr for eight days. It was then

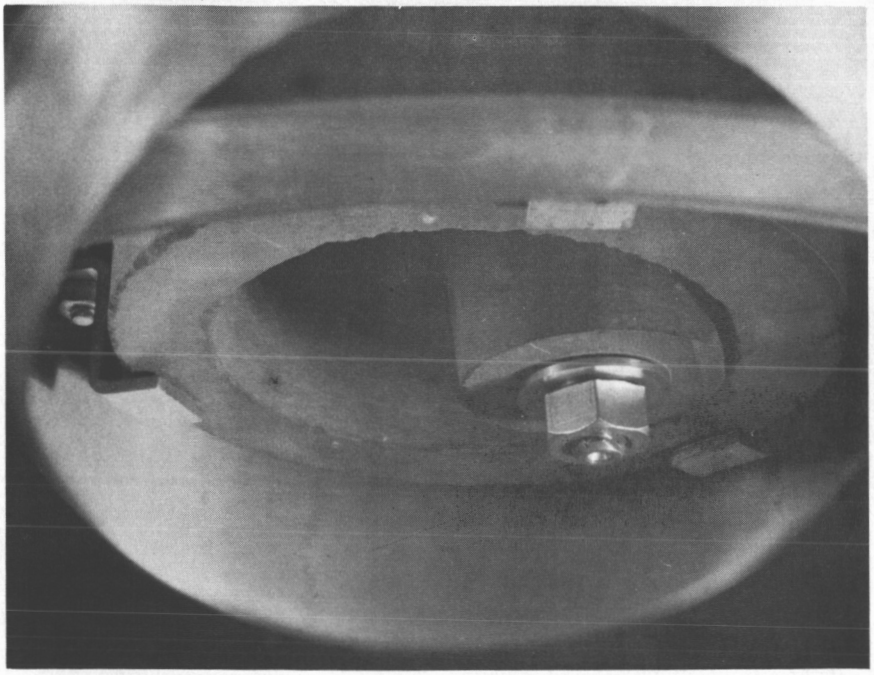

FIG. 10. Rock grinding components before vacuum grinding.

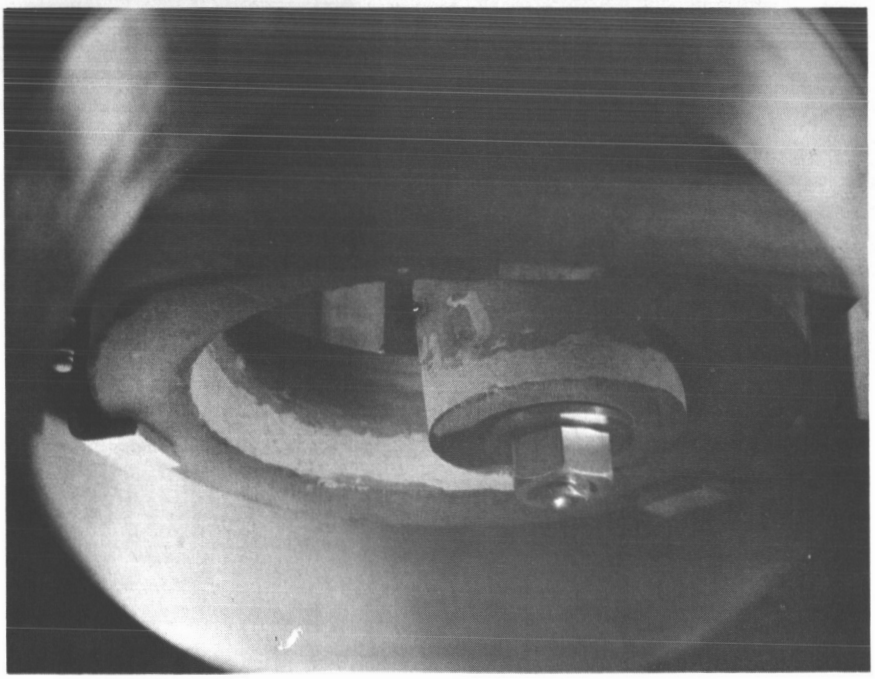

FIG. 11 Rock grinding components after 1-1/2 hours of vacuum grinding.

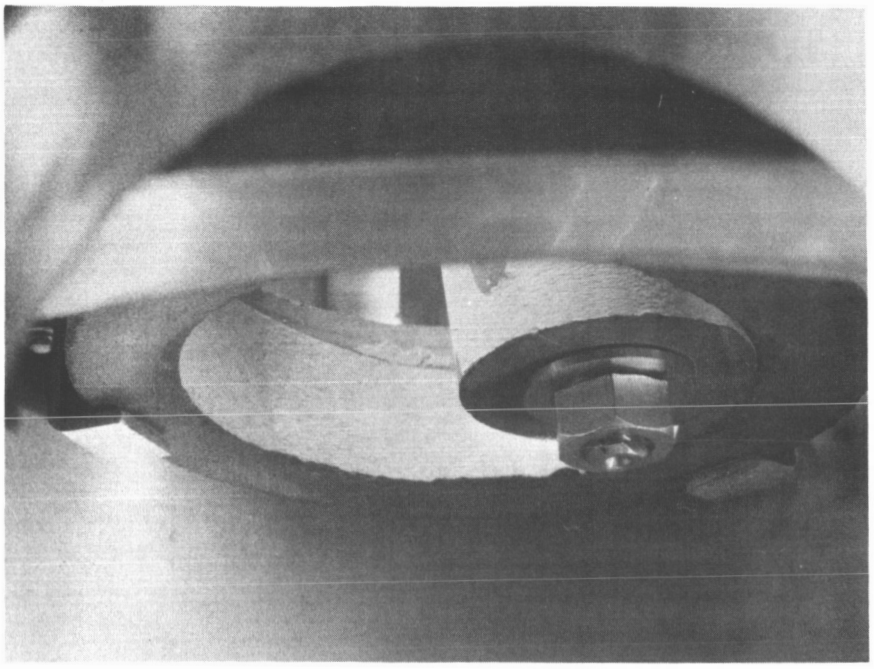

FIG. 12. Rock grinding components after 17 hours of vacuum grinding.

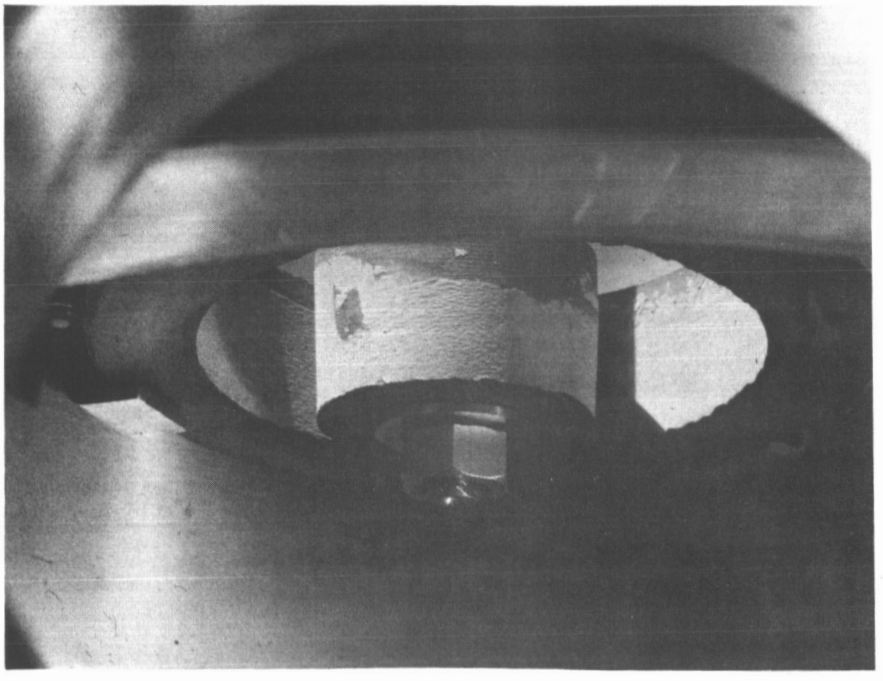

FIG. 13. Rock grinding components after 17 hours of vacuum grinding.

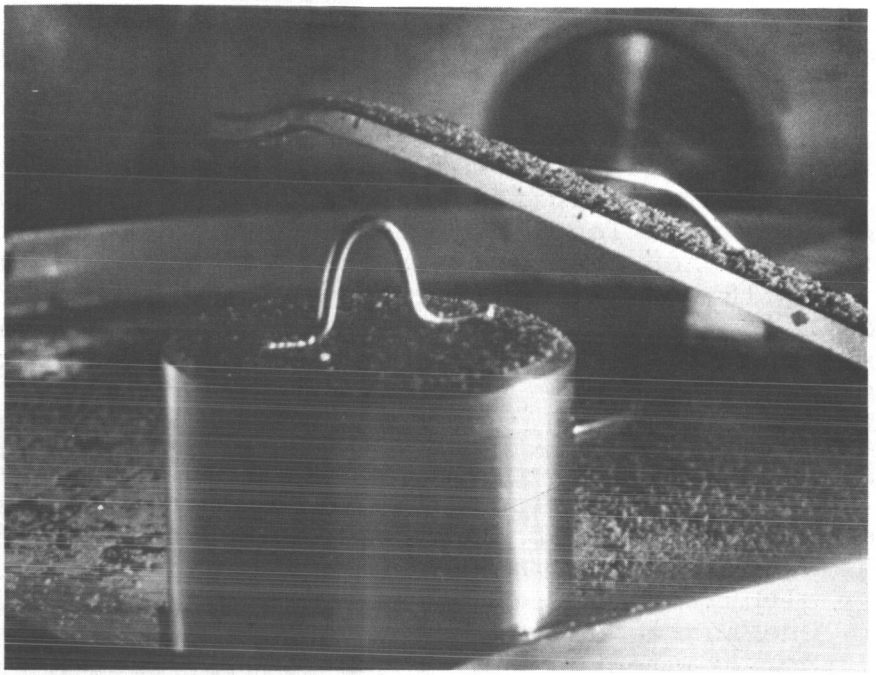

FIG. 14. Collecting pan, manipulator, and weight after vacuum grinding.

vented to atmospheric pressure with nitrogen. No visible alteration of the powder was evident either after vacuum storage or after venting.

Fig. 15 shows a close up of part of the abrading wall of the outer component. The view is from above the rock in air. Powder both on and above the rock grinding interface is evident. The amount of powder sticking in these two areas was one of the most significant differences between air ground and vacuum powders. A similar view is shown in Fig. 16 after grinding in air for the same length of time. In air no material adhered above the grinding area and a far thinner amount of powder clung to the grinding interfaces themselves.

Fig. 17 shows a flake of adherent powder about 1/7 inch in diameter which was lifted from above the grinding area. As is evident, the flake is sufficiently strong to support itself when resting on a wire loop. The same effect was observed with powder on the pan when compressed by the 200 gram weight to 0.32 psi. Fig. 18 shows a flake from the area over which the weight slid, being lifted with a scalpel. The latter effect was also approached using air ground powder, but a thicker specimen was required.

Fig. 19 shows a view of the pan near where the weight slid to rest. A variety of powder aggregates are evident, especially at the top of the picture along side the lip of the straight part of the pan. Several of the larger ones are 1/8 inch in length. The angularity of many of the pieces is especially notable. It gives the aggregates as a group a gravel-like appearance. One aggregate was 1/4 inch long and was mistaken for a rock fragment. When intentionally broken with a pair of tweezers it divided into two intact components having noticeably greater firmness than displayed by aggregates produced by air grinding. The shape and size of the aggregates shown in Fig. 19 indicates their formation from free powder rather than from the compression of powder as were the flakes shown in Figs. 17 and 18.

Aggregates were also produced in air but constituted a smaller powder fraction than those produced in vacuum. Most significantly, however, is the almost uniformly spherical shapes of the aggregates as opposed to the more diverse and angular shapes produced in vacuum. Fig. 20, a close-up of some of the air-ground powder alongside the lip of a curved part of the pan, illustrates this phenomenon; the primary exceptions are the small flakes from the rock grinding interfaces. Both air ground and vacuum ground powders do have an identical appearance in the funnel shaped collecting cups, however. Fig. 21 shows the shperical aggregates formed there by the vacuum ground powder. They are attributed to contamination as particles strike the funnel sides before hitting the bottom. The shperical shapes are similar to the "dancing" aggregates observed in vacuum which were described earlier.

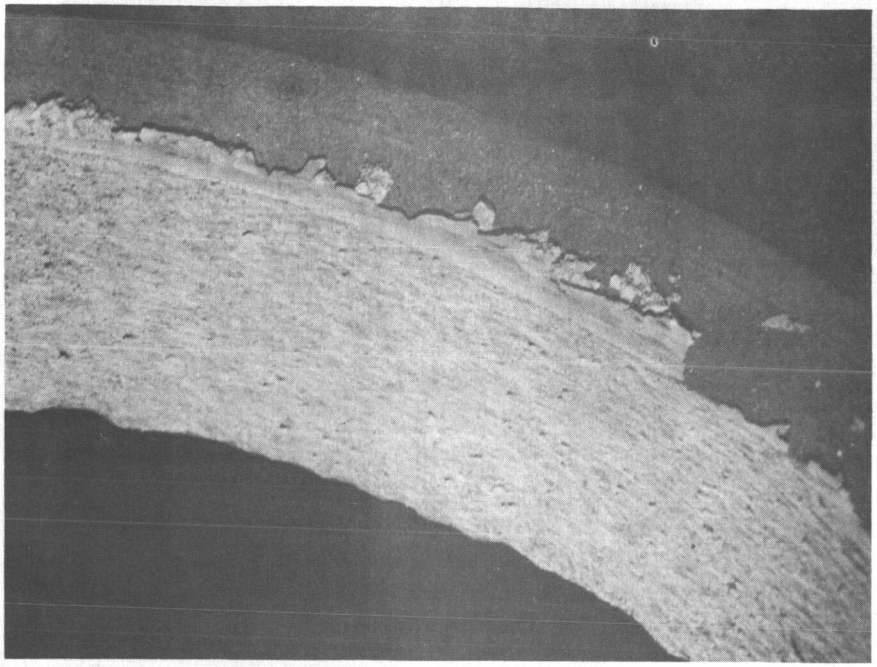

FIG. 15. Close-up of the abrading wall of the outer rock after vacuum grinding; view is from above.

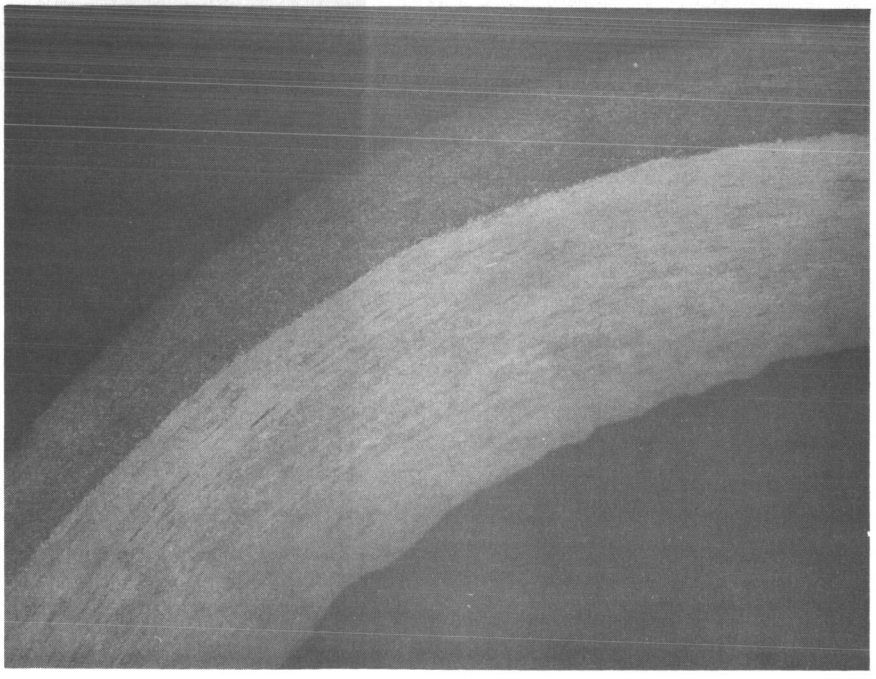

FIG. 16. Close-up of the abrading wall of the outer rock after air grinding; view is from above.

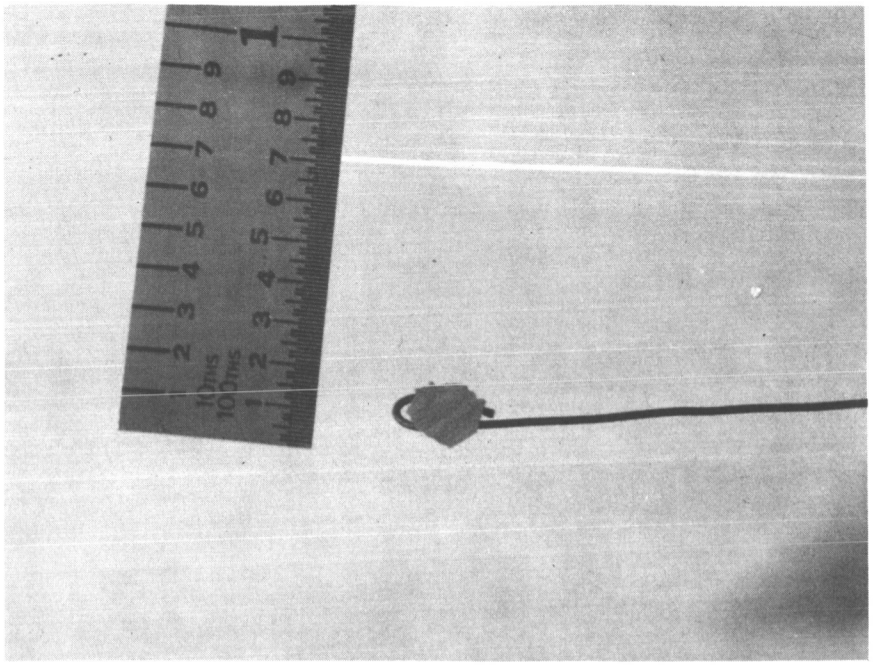

FIG. 17. Self supporting flake of powder taken from above the rock grinding interface, after vacuum grinding.

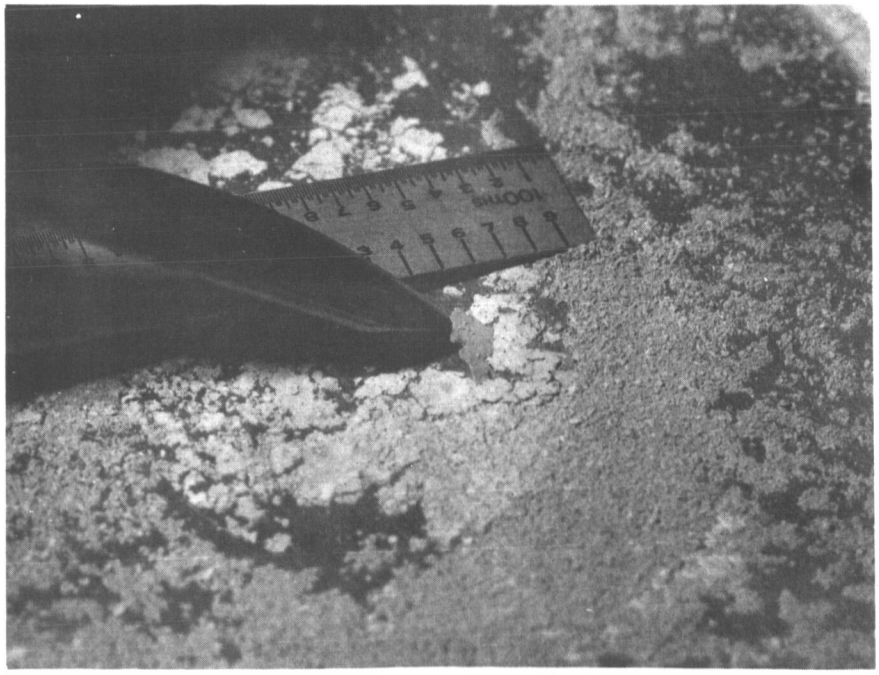

FIG. 18. Self supporting flake of powder resulting from compression of free powder on the pan after vacuum grinding.

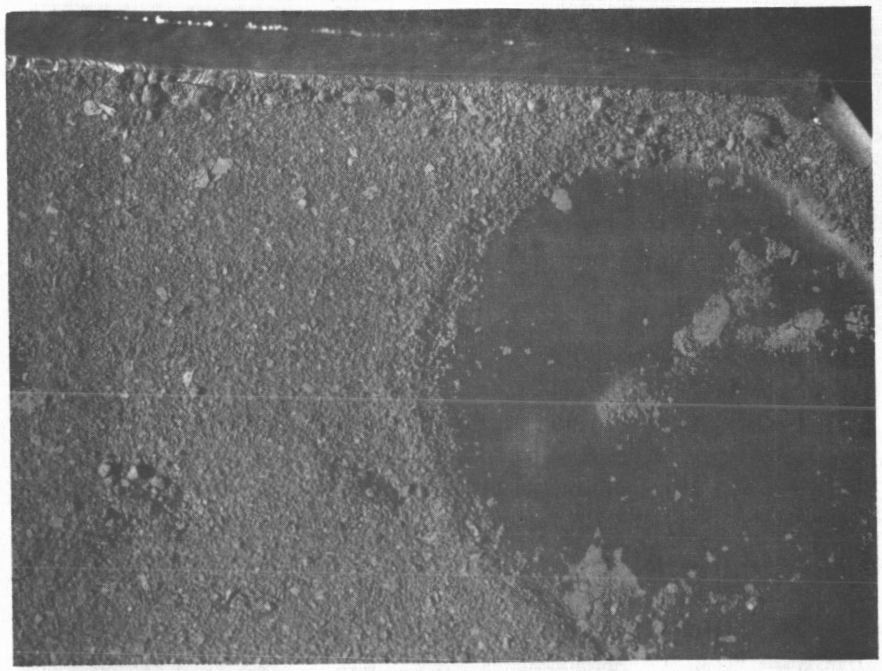

FIG. 19. Angular shaped appregates produced in the collecting pan by vacuum grinding.

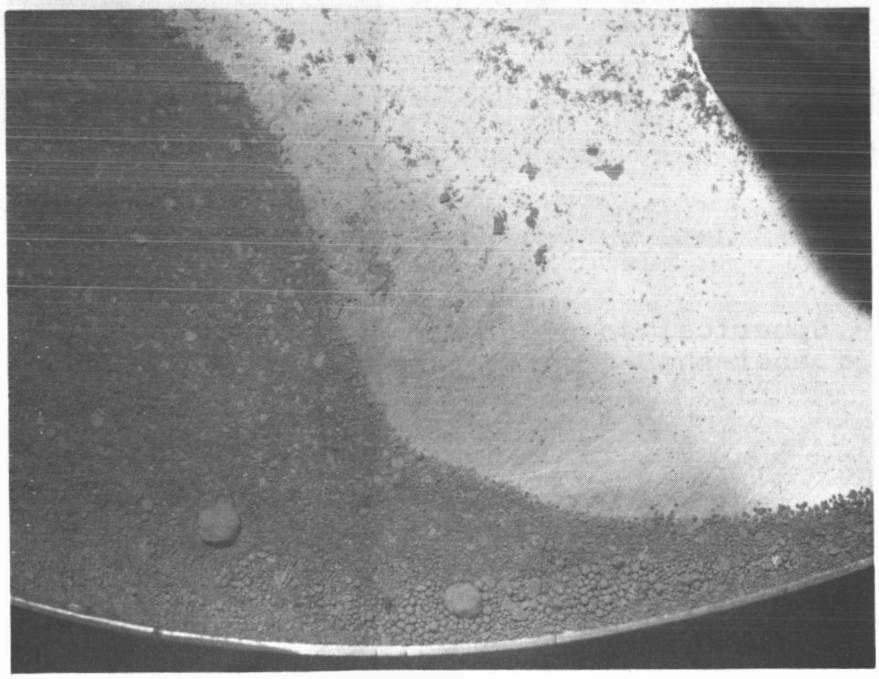

FIG. 20. Spherical shaped aggregates produced in the collecting pan by air grinding.

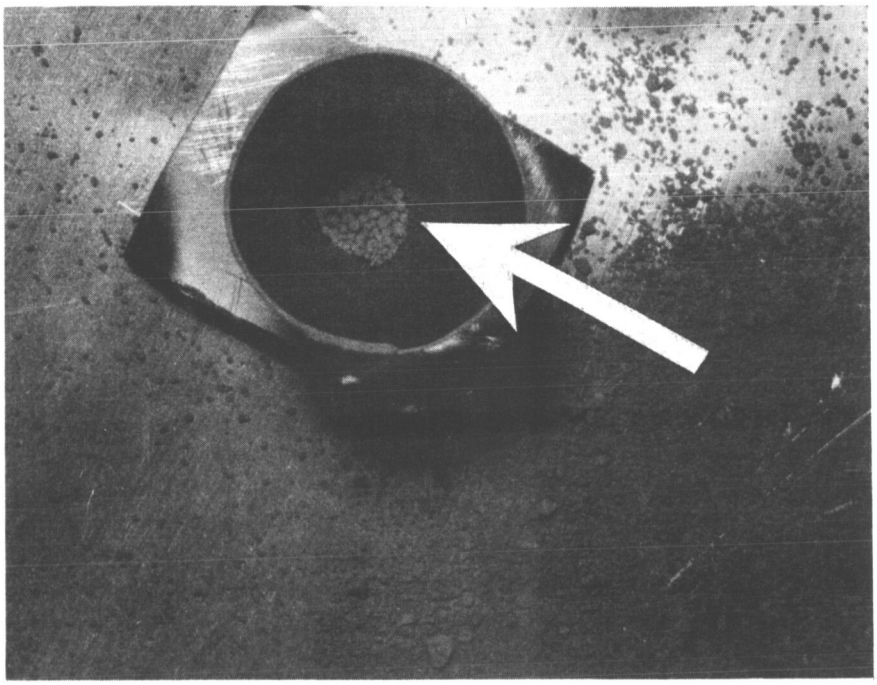

FIG. 21. Spherical shaped aggregates (arrow) produced in the funnel-shaped collecting cup after vacuum grinding.

Fig. 22 shows the vacuum-ground powder distribution over the entire collecting pan; the pan is circular with an 8 inch diameter except for the straight portion shown at the top. The powder distribution is essentially undisturbed from its appearance in vacuum. The general gravel-like appearance is again evident. The circular, sparsely powdered area to the left and above the center of the pan was beneath the hollow area of the outer rock. The circular wire at the bottom of this region held the weight before it was placed on fallen powder. The component to its left is a thin metal bridge; little powder stuck to it for reasons not known. Areas of the pan shown enlarged in previous figures are outlined with dashes. Above the bridge is the funnel shaped collecting cup. To the right of the circular wire is the smeared powder produced by the sliding weight. At the upper right is where the weight piled some powder into a semi-circular ridge.

Fig. 23 shows the pan containing powder ground in air after the same grinding duration as in vacuum. More powder was formed than in vacuum and may partially account for some of the differences observed. The circular pattern about a sparcely coated area, which outlined the grinding perimeter in the vacuum-ground powder, is missing indicating air-ground powder to be less adherent to the pan and more responsive to pan vibrations. Vibrations have also set up waves (arrows) indicating less powder self adherence, as well. Air ground powder generally appears more sand-like and less gravel-like than vacuum-ground powder. The area previously illustrating the spherical aggregates is outlined with dashes.

A single aggregation of vacuum ground powder was found smeared into a large crevise in the outer rock's grinding interface (referred to earlier). The aggregation was about 1/2 inch in its largest dimension and about 3/16 inch at its deepest. The roughness of the surface may have assisted in maintaining the powder as a unit by retarding its movement. Unfortunately, the counterpart for air ground powder was overlooked.

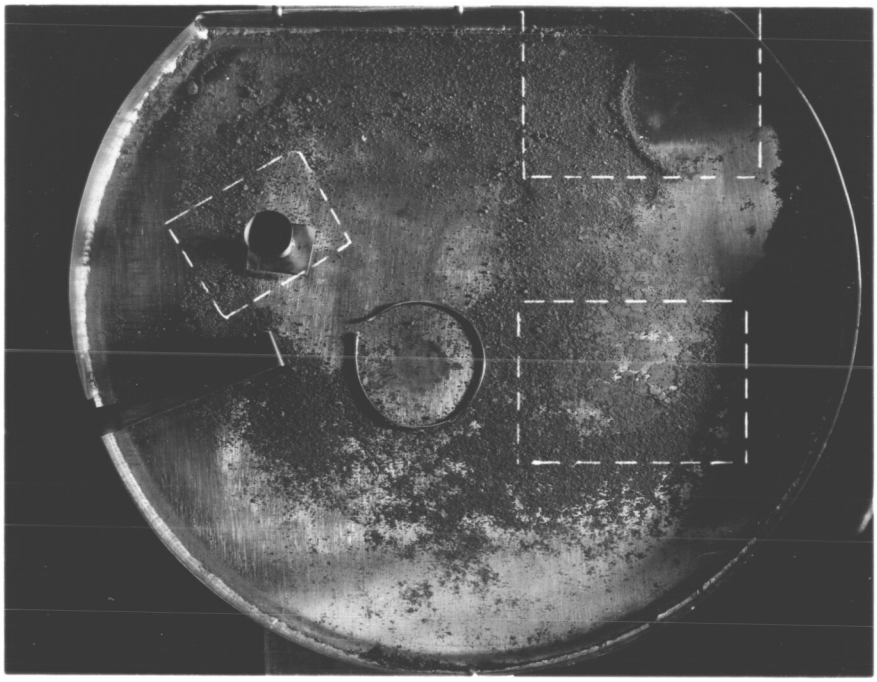

FIG. 22. Over-view of powder on the collecting pan after vacuum grinding. Dashes outline areas shown enlarged in previous figures.

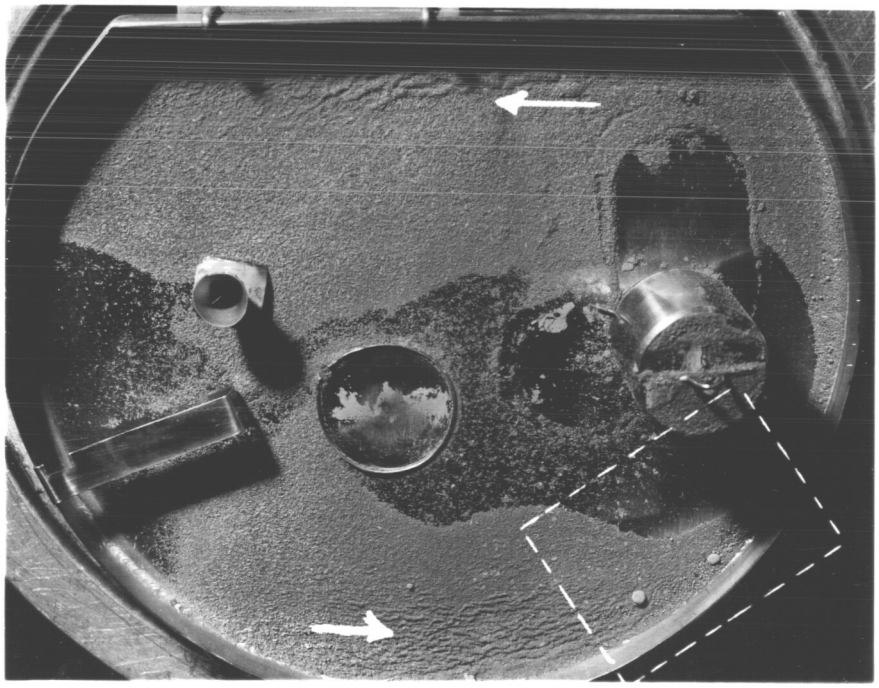

FIG. 23. Over-view of powder on the collecting pan after air grinding. Dashes outline area previously shown enlarged, arrows indicate waves.

Powder production rate, size distribution and microscopic appearance. - Approximately 0.9 grams of powder was produced during the 17 hours of vacuum grinding or 0.5 grams per hour. This was 1/4 the production rate of the air ground powder.

The bulk of both the air ground and the vacuum ground particles were in the micron range or below. Particles were therefore magnified with an electron microscope and photographed to examine them for differences in shape, size, method of microscopic adhesion, etc. Vacuum-ground specimens were taken from above the rock grinding interfaces, air ground from the pan. Representative pictures are shown at 13,000 times magnification in Figs. 24 and 25. Except for size, no obvious differences between the two types of powder are discernible.

Table III shows the particle size distributions, which were determined from electron microscope photographs; both the percentage of the number of particles in each size range and the percentage of the weight of the particles in each size range are tabulated. This was done for both air-ground and vacuum-ground powder. A size of .05μ was the lower limit with which particles could be clearly discerned. The vacuum-ground particles are seen to have a greater percentage of large sizes, which may be quite significant. However, it may be due to greater aggregation in vacuum; while efforts were made to count individual particles, aggregates sometimes may have been counted by mistakes. Further experimentation would be necessary definitely to sustain the differences noted. The vacuum-ground particle sizes were distributed such that 50% of the particles were above 0.5μ, while 50% of their weight was above 1.5μ.

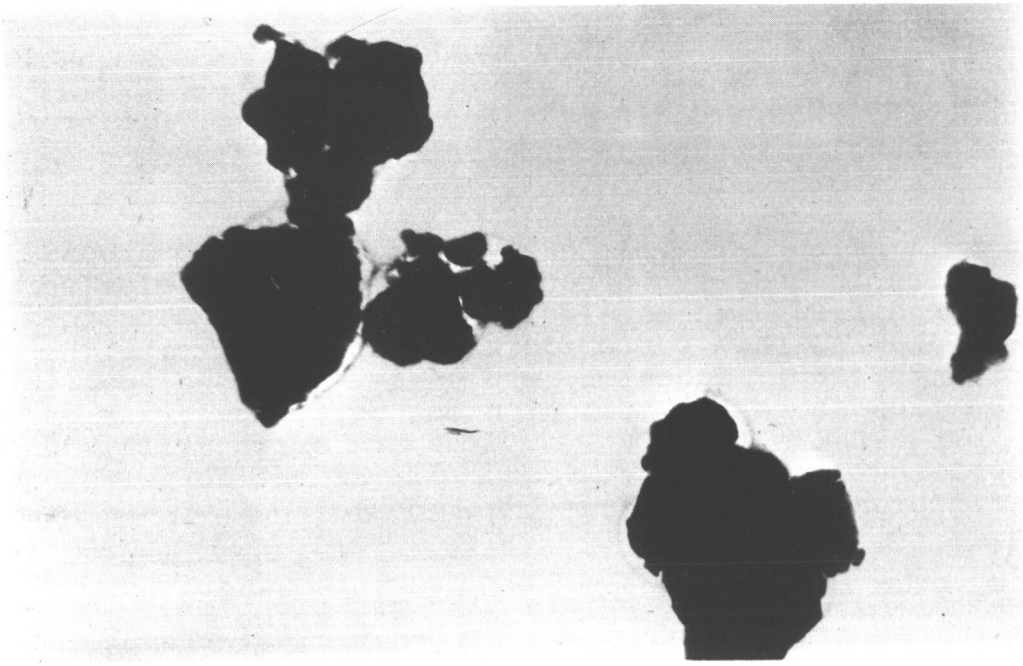

FIG. 24. Vacuum ground basalt particles magnified 13,000 times.

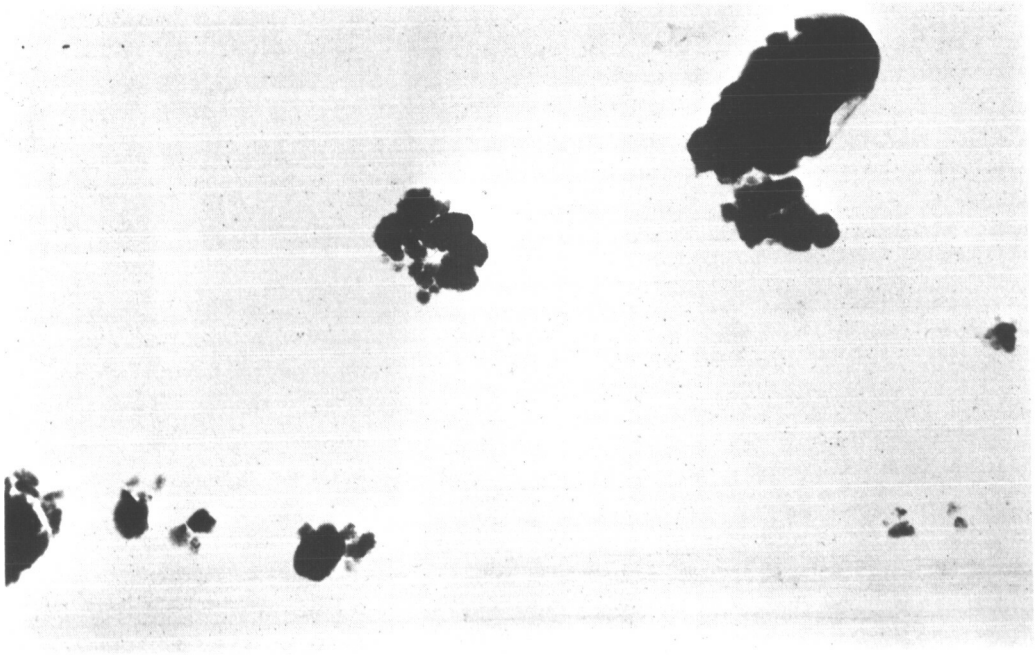

FIG. 25. Air ground basalt particles magnified 13,000 times.

Table III. Percent Size Distribution by Number and by Weight of Particles

Distribution Type	Size Range (μ)		
	.05-.2	.2-.8	.8-3
Air No.	47	45	8
Vacuum No.	15	50	35
Air Wt.	4	35	61
Vacuum Wt.	<1	13	87

CONCLUSIONS AND DIRECTION OF FUTURE WORK

Simulation of lunar soil surface cleanliness by UHV igneous rock comminution is concluded feasible. Rock prebaking at atmosphere, using high temperatures for long durations, appears to be an essential preparation. The 0.66% weight reduction resulting from the thermal treatment evidences the contaminability of the rock powder with gas from the rock itself, especially in atmospheres higher than UHV; this includes inert atmospheres. The low 10^{-9} and 10^{-8} Torr pressures maintained during grinding could probably be lowered to the low 10^{-10} Torr range with more extended baking. This would be desirable for even closer simulation of the lunar environment.

Due to the adherence of vacuum ground powder to the rock grinding interfaces, the release of gas produced during comminution was evidently slowed; the drop in chamber pressure as grinding proceeded supports this conclusion. This probably caused some degree of contamination and a consequent decrease in adhesion over that which otherwise would have existed. Means for allowing powder removal from the interfaces during grinding would therefore be a beneficial improvement. It would also increase the powder production rate and eliminate powder compression and stirring, which serve to complicate interpretation of results. The use of a coarse diamond wheel in place of the center rock component may be a beneficial improvement to this end.

The powder apparently falls in an essentially predictable vertical manner and tends to stick where it falls. Collection for quantitative testing can therefore be expected to be straight-forward. However, the spherical aggregates formed in the funnel indicate that funneling or other means of forcing repeated contacts with metal surfaces, even though the latter are baked, contaminate the powders and should be avoided. A compact collection method is required where powder can accumulate directly in the place to be tested.

Rock powder produced under conditions simulating the lunar vacuum environment has greater self adhesion and greater adhesion to solid rock and to metal surfaces than powder produced at atmosphere. This was evidenced, both for free powder and powder that was compressed, by a variety of adhesive forms and locations. Especially notable was the compressed powder adherent to the vertical rock walls above the grinding interface, from which self supporting flakes could be removed, and the uncompressed powder adherent to the underside of the rocks. No air ground counterparts existed. The angular, gravel-like aggregates formed of uncompressed powder on the pan, as opposed to the spherical shaped aggregates formed there in air, was another important indicator. It suggests that many of the "rocks" appearing on the Surveyer and Ranger photographs may, in fact, be powder aggregates. The larger size distribution indicated for vacuum ground particles is also interesting and may be worth further investigation. It may indicate a smaller amount of comminuted rock on the lunar surface than has been estimated.

Quantitative measurements of powder strength in vacuum are now required along with improvements in the comminution and collection method. Investigation has shown direct shear testing to be suitable to this end. This testing method and the manner in which information is derivable from it is briefly described in the Appendix. It has previously been used in vacuum by Vey and Nelson.[14] It has the advantage of requiring a small specimen (about 20 cm^3) and is capable of providing an abundance of basic soil engineering information, including shear strength versus normal load, coefficient of friction, and cohesion. From this basic information other characteristics can be derived including bearing capacity as a function of footing size and other pertinent parameters. The direct shear test would also allow a means for investigating the nature of the forces involved in the powder adhesion.

APPENDIX: DIRECT SHEAR TESTING

The direct shear apparatus employs a cylindrical container filled with soil. The container is separated into two parts about its perimeter as shown in Fig. 26. One half is moved horizontally relative to the other along a shearing plane. Normal loading is applied to the soil by means of a piston. The shear strength of the material is determined from the lateral force required to move the containers apart. Shear strength vs. normal load results in a straight line described by

$$s = c + \sigma \tan\phi \qquad (2)$$

from which is obtained the shear strength s, as a function of normal force σ, the angle of internal friction ϕ, the coefficient of friction s/σ, and the cohesion of the soil c, which is the no-load shear strength.

This basic soil information allows other characteristics to be determined, including the soil's bearing capacity[15], q_o, as a function of pertinent parameters. This is determinable from

$$q_o = \gamma b N_\gamma / 2 + c N_c + q' N_q \qquad (3)$$

where b is the width of the bearing foot (if circular), γ is the soil density, c is the cohesion, q' is the soil pressure adjacent to the area being loaded and N_γ, N_c and N_q are known quantities which depend on the angles of internal friction ϕ.

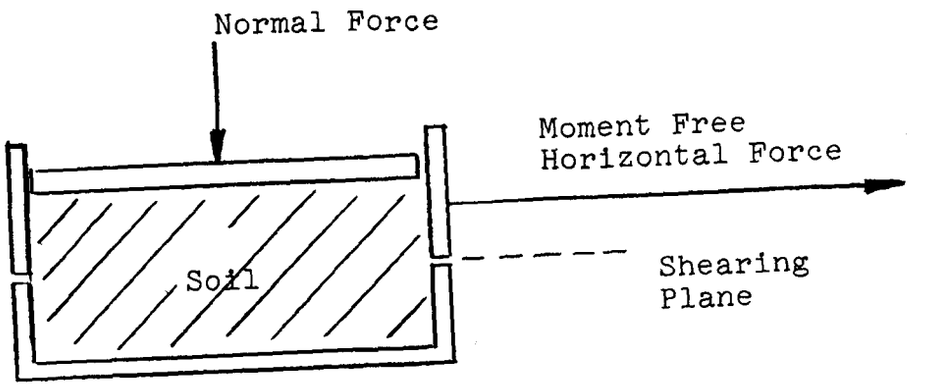

FIG. 26. Schematic of shear test soil container.

REFERENCES

1. Salisbury, J.W.; et al: Adhesive Behavior of Silicate Powders in Ultrahigh Vacuum. J. Gesophys. Res., vol 69. no. 2, Jan. 1964, pp.235-242.

2. Halajian, J.D.: Soil Behavior in a Low and Ultrahigh Vacuum. Paper presented at Aviation and Space Division Winter Annual Meeting, Am. Soc. Mech. Engrs. (New York, N.Y.), Nov-Dec., 1964.

3. Vey, E; and Nelson, J.D.: Engineering Properties of Simulated Soils. J. Soil Mech. Found. Div., Proc. Am. Soc. Civil Engrs., vol.91, no. SM1, Proc. Paper 4199, Jan. 1965, pp. 25-52.

4. Bernette, E.C.; et al: Bearing Capacity of Simulated Lunar Surfaces in Vacuum. Am. Inst. Aeron. Astronaut.J., vol. 2, no. 1, Jan. 1964, pp. 93-98.

5. Wong, R.E.; and Kern, C.: Test Program for Determination of Soil Constants in Vacuum. Paper presented at Aviation and Space Division Winter Annual Meeting, Am. Soc. Mech. Engrs. (New York, N.Y.), Nov.-Dec. 1964.

6. Ham, J.L.: Metallic Cohesion in High Vacuum. Am. Soc. Lubrication Engrs. Trans., vol. 6, 1963, pp. 20-28.

7. Bell, P.R.: Vacuum Welding of Olivine. Science, vol. 153, no. 3734, July 1966, pp. 410-411.

8. Ryan, J.A.: Adhesion of Silicates in Ultrahigh Vacuum. J. Geophys. Res., vol. 71, no. 18, Sept. 1966, pp. 4413-4425.

9. Rosenberg, D.L.; and Wehner, G.K.: Darkening of Powdered Basalt by Simulated Solar-Wind Bombardment. J. Geophys. Res., vol. 69, no. 15, Aug. 1964, pp. 3307-3308.

10. Green, J.: The Lunar Prospect, in Appollo-A Program Review. Paper presented at Nat. Aeron. Space Eng. Mfg. Meeting, Soc. Auto. Engrs., Proc. SP-257 (Los Angeles, Calif.), Oct. 1964, pp. 113-124.

11. Salisbury, J.W.: op. cit.

12/5/67

12. Lyon, R.J.P.: Evaluation of Infrared Spectrophotometry for Compositional Analysis of Lunar and Planetary Soils, Part II. NASA CR-100, 1964.

13. Spock. L.E.: Guide to the Study of Rocks. Second ed., Harper and Row, 1962, p. 101.

14. Vey, E.; and Nelson, J.D.; op. cit.

15. Sowers, G.B.; and Sowers, G.F.: Introductory Soil Mechanics and Foundations. Second ed., Macmillan Co., 1961, p.156.